Theoretical study on the phase stability, site preference, and lattice parameters for Gd(Fe, T)$_{12}$

2001 J. Phys.: Condens. Matter 13 2727

(http://iopscience.iop.org/0953-8984/13/11/326)

INSTITUTE OF PHYSICS PUBLISHING JOURNAL OF PHYSICS: CONDENSED MATTER

J. Phys.: Condens. Matter **13** (2001) 2727–2736 www.iop.org/Journals/cm PII: S0953-8984(01)17143-2

Theoretical study on the phase stability, site preference, and lattice parameters for Gd(Fe, T)$_{12}$

Chen Nan-xian[1,2,3,4,6], **Shen Jiang**[3,4] **and Su Xuping**[3,4,5]

[1] China Centre of Advanced Science and Technology (World Laboratory), PO Box 8730, 100080, China
[2] Department of Physics, Tsinghua University, 100084, China[7]
[3] Institute of Applied Physics, Beijing University of Science and Technology, 100083, China
[4] National 863 Laboratory for Materials Modelling and Design, Beijing 100083, China
[5] Material Engineering Department, Xiangtang University, Hunan 411105, China

Received 14 September 2000, in final form 22 January 2001

Abstract

The stability of the intermetallics Gd(Fe, T)$_{12}$ and the site preferences of the ternary 3d or 4d transition element T are investigated by using a series of interatomic pair potentials, $\Phi_{\mathrm{Fe-Fe}}(r)$, $\Phi_{\mathrm{Fe-Gd}}(r)$, $\Phi_{\mathrm{Fe-T}}(r)$, $\Phi_{\mathrm{T-T}}(r)$, $\Phi_{\mathrm{T-Gd}}(r)$, and $\Phi_{\mathrm{Gd-Gd}}(r)$, for the first time. The calculated results show that adding either Cr, Mo, Ti, or V atoms makes the crystal cohesive energy of Gd(Fe, T)$_{12}$ decrease markedly, proving that these atoms can stabilize Gd(Fe, T)$_{12}$ with ThMn$_{12}$ structure even though the GdFe$_{12}$ crystal structure is itself metastable. The calculated lattice parameters are in good agreement with experiment. The amount of cohesive energy decrease is correlated with the species and occupation site of the ternary atoms. The order of site preference of these stabilizing elements T is 8i, 8j, and 8f, with 8i corresponding to the greatest energy decrease. The calculated results further show that the addition of Co, Cu, Ni, Sc, and Zn does not stabilize the GdFe$_{12}$ phase in the ThMn$_{12}$ structure. The calculated results reported correspond well to available experimental data indicating that the *ab initio* interatomic potentials can be used to describe rare-earth materials.

1. Introduction

In 1981, Yang *et al* discovered the Y(Mn$_{1-x}$Fe$_x$)$_{12}$ intermetallic compounds that have the ThMn$_{12}$ structure for a large range of iron content [1]. In 1987, de Mooij and others discovered the Fe-rich compound RFe$_{10}$V$_2$ (R = Y, Ce, Nd, Sm, Gd) with the ThMn$_{12}$ structure, and, subsequently, other series of rare-earth compounds with this structure have been obtained [2,3]. These compounds have high Curie temperatures, and some of them have large magnetic moments indicating that they may be valuable as permanent magnets. In fact, the binary compounds RFe$_{12}$ are metastable, but when a moderate amount of a ternary element T (T = Cr,

[6] Author to whom any correspondence should be addressed.
[7] Mailing address.

Mo, Ti, V, or Si) is added, R(Fe, T)$_{12}$ can be stable. The ternary element therefore obviously plays a role in structural stabilization. The lattice cell of RFe_{12} is shown in figure 1 [2]. It belongs to the space group $I4/mmm$, and consists of 26 atoms, or two RFe_{12} formula structures, with four distinct kinds of site. Rare-earth atoms occupy 2a sites, and Fe atoms occupy the 8i, 8j, and 8f sites. According to x-ray diffraction analysis, most stabilizing elements, T, such as V, Mo, or Cr, preferentially substitute for the Fe atom at i sites [4, 6–10]. For example, Cr, Mo, and V preferentially occupy 8i sites, and Ti preferentially occupies 8i + 8j sites.

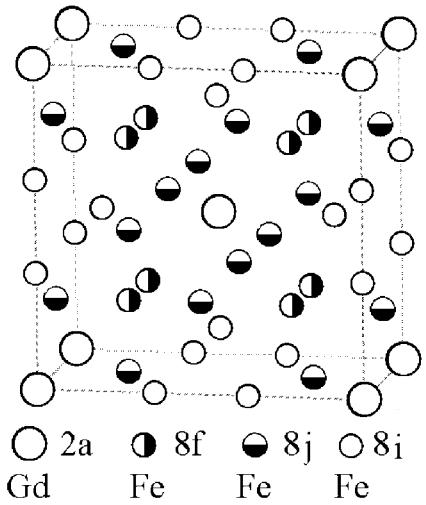

Figure 1. The lattice cell of $GdFe_{12}$. The y-axis is vertical, and the z-axis is horizontal, pointing to the right. The origin is located at the south-west corner.

In this paper, a series of interatomic pair potentials in Gd(Fe, T)$_{12}$ are determined by using a general lattice-inversion technique and a first-principles-based crystal cohesive energy calculation. In this way, the stability of Gd(Fe, T)$_{12}$, and the T-site preferential occupation are evaluated and analysed. The calculated results are in good agreement with existing experimental results for all 3d additions, and the results with 4d additions for $GdFe_{12-x}T_x$ are calculated as predictions for future experimental work. Section 2 gives an introduction to the methodology for the calculation. Section 3 shows the calculated results and gives a comparison to experiment. Section 4 gives an intuitive explanation of the calculated results based on the picture of interatomic potentials. The conclusions and a discussion are given in section 5.

2. Methodology

The technique used for obtaining the *ab initio* pair potential was initially proposed by Carlsson *et al* [11]. However, the expression for their solution includes infinite summations, each of which includes infinite terms, making it inconvenient for analysis.

2.1. Chen's lattice-inversion technique

The most naive model for solid cohesion expresses the total cohesive energy per atom of a solid, E, in terms of the sum of interatomic pair potentials, $\Phi(R_i)$. The latter depends only upon the distance r_i between a representative atom at the origin and another atom i. If the

energy is known as a function of volume, or equivalently the nearest-neighbour distance, x, then the inverse problem is that of inverting the pair potential, $\Phi(x)$, in terms of $E(x)$ on the basis of the following expression [12–17]:

$$E(x) = \frac{1}{2}\sum_{R_i \neq 0} \Phi(R_i) = \frac{1}{2}\sum_{n=1}^{\infty} r_0(n)\Phi(b_0(n)x) \tag{1}$$

where x is the nearest-neighbour distance, R_i is the position vector of the ith atom, $b_0(n)x$ is the nth-neighbour distance, and $r_0(n)$ is the nth coordination number. We extend the series, $\{b_0(n)\}$, into a multiplicative semi-group such that, for any two integers m and n, there always exists an integer k such that

$$b(k) = b(m)b(n). \tag{2}$$

Equation (1) can then be rewritten as

$$E(x) = \frac{1}{2}\sum_{n=1}^{\infty} r(n)\Phi(b(n)x) \tag{3}$$

where

$$r(n) = \begin{cases} r_0(b_0^{-1}[b(n)]) & \text{if } b(n) \in \{b_0(n)\} \\ 0 & \text{if } b(n) \notin \{b_0(n)\}. \end{cases} \tag{4}$$

Thus the pair potential, $\Phi(x)$, can be written as

$$\Phi(x) = 2\sum_{n=1}^{\infty} I(n)E(b(n)x) \tag{5}$$

where $I(n)$, the inversion coefficient, can be uniquely determined from the crystal structure as

$$\sum_{b(n)|b(k)} I(n)r\left(b^{-1}\left[\frac{b(k)}{b(n)}\right]\right) = \delta_{k1}. \tag{6}$$

Note that this inversion coefficient $I(n)$ is only structure dependent; thus repeated calculation is not needed for different materials belonging to the same crystallographic structure group.

2.2. The first-principles calculation

In this work, the whole process is carried out within a first-principles framework, increasing the reliability of the results, and is especially favourable for study of series. To reduce the time requirement, the calculations of $E(x)$ are performed on the basis of an *ab initio* augmented-spherical-wave method [19–22] within the local density functional theory, even though other *ab initio* methods, such as the norm-conserving pseudopotential technique, may provide better results in some cases. The cohesive energy is obtained from

$$E(x) = E_{tot}(x) - E_{tot}(\infty). \tag{7}$$

A series of functions $E(x)$ are calculated with various lattice constants at equal intervals of 0.1 Å. In each case, for generating the total energy, more than 80 k-points in an irreducible Brillouin zone are taken into account in a self-consistent calculation. The data are then fitted on the basis of Rose functions [23]. This is quite an standard procedure in calculations using an Origin 2000 machine, and ESOCS code from MSI (Materials Simulation Incorporation).

To give an intuitive impression, some of the calculated interatomic potentials are shown in figure 2.

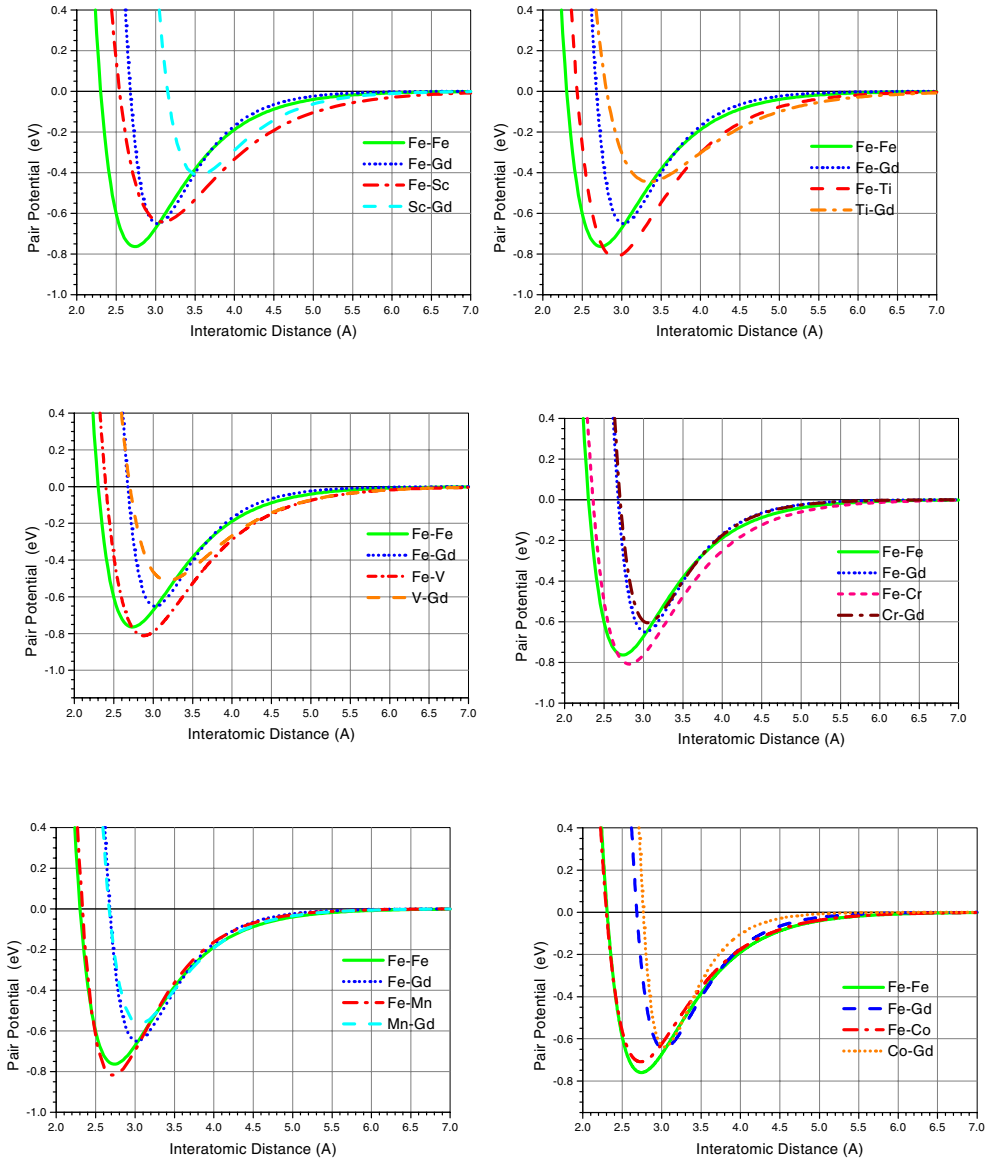

Figure 2. Some important interatomic potentials.

3. The calculation procedure and results

In this paper, the structure and cohesive energy of a periodic supercell with 208 atoms, or $RFe_{12-x}T_x$ undergoing relaxation, are studied on the basis of calculated interatomic potentials. Energy minimization, rather than molecular dynamics simulation, is carried out using the conjugate-gradient method with MSI software with the cut-off distance of 14 Å. The energy values for $(RFe_{12-x}T_x)_{16}$ in figure 3 are the results of taking the arithmetic average for 20 stochastic samples produced by random substitution of ternary additions for Fe. The error bars in the figure represent the ranges of the root mean square errors.

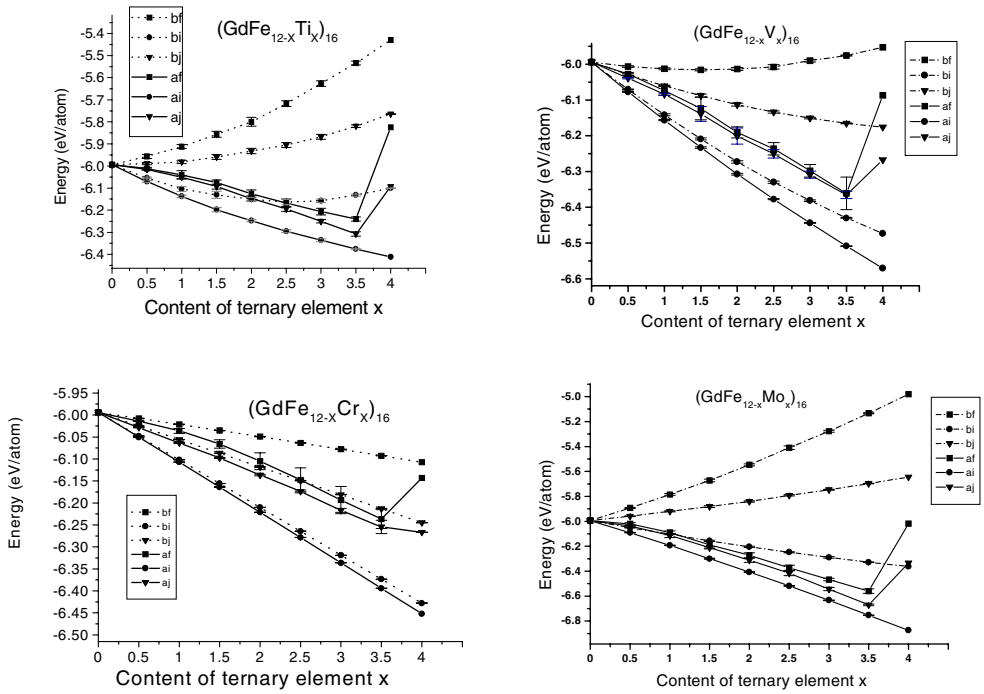

Figure 3. The effect of ternary elements on the phase stability and site preference for unrelaxed cases (a) and for relaxed cases (b).

3.1. Calculation of the structure parameters

3.1.1. The intrinsic structure. The virtual binary structure $GdFe_{12}$ can be considered as the intrinsic structure of the pseudo-binary compounds Gd(Fe, T)$_{12}$, even though it is metastable. In the calculation, the initial lattice parameters of $GdFe_{12}$ are set arbitrarily (see table 1), and the conjugate-gradient method is used to minimize the system energy on the basis of the calculated interatomic potentials. This is essentially a quasi-static process of dynamic relaxation evolution. The result indicates that the final stabilized structure is tetragonal with

Table 1. Determination of lattices parameters of $GdFe_{12}$.

Initial (unrelaxed)		Final (relaxed)	
a, b, c (Å)	α, β, γ (deg)	a, b, c (Å)	α, β, γ (deg)
8.496, 8.496, 4.76	90, 90, 90	8.428, 8.428, 4.798	90, 90, 90
2, 2.5, 3	92, 88, 90	8.428, 8.428, 4.798	90, 90, 90
12, 12, 12	90, 90, 90	8.428, 8.428, 4.798	90, 90, 90
2, 2, 2	70, 70, 70	8.428, 8.428, 4.798	90, 90, 90
10, 10, 10	88, 88, 88	8.428, 8.428, 4.798	90, 90, 90
8, 8, 5	60, 60, 60	8.428, 8.428, 4.798	90, 90, 90
16, 16, 10	90, 90, 90	8.428, 8.428, 4.798	90, 90, 90
1, 1, 1	90, 90, 90	8.428, 8.428, 4.798	90, 90, 90
1, 1, 1	88, 88, 88	6.6, 7.78, 6.96	85.7, 94.3, 94.30
1, 4, 1	60, 70, 70	6.765, 8.184, 6.355	84.5, 87.9, 84

space group $I4/mmm$. The atom site occupations agree with the $ThMn_{12}$ structure, and the lattice constants are stabilized at $a = 8.428$ Å and $c = 4.798$ Å provided that both the symmetry and the size of the lattice constants of the initial model are very close to the values known for Gd(Fe, T)$_{12}$ (table 1). The calculated lattice constants of $GdFe_{12}$ are close to the experimental values for Gd(Fe, T)$_{12}$ intermetallics [4–6], demonstrating that the structure of $GdFe_{12}$, though metastable, is close to that of a stable phase.

3.1.2. The ternary systems. The dependence of the lattice constants on the content of ternary addition is illustrated in figure 4, showing the slow variation of the lattice constants as the content of the ternary additions increases for the 8i-site substitution. Table 2 shows that the calculated results are in good agreement with experiment, with an average deviation less than 0.33%, the largest being 0.93%.

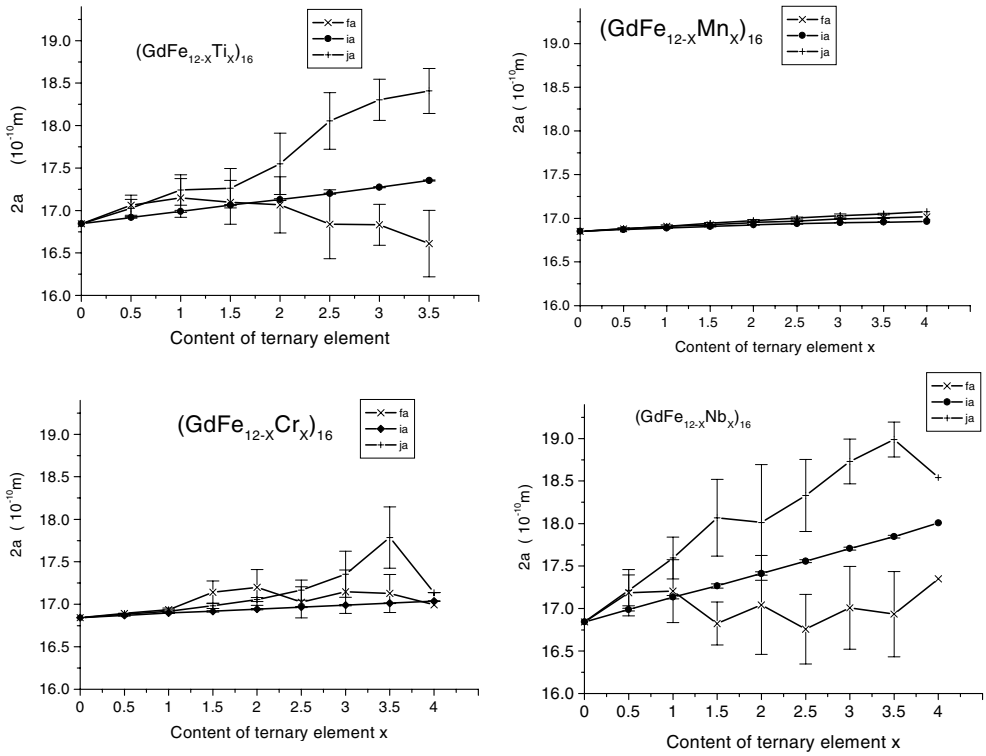

Figure 4. The dependences of the lattice constants on the content of ternary additions.

Table 2. The comparison between calculated and experimental lattice parameters [24] (in Å).

	Calculated a (Å)	Experimental a (Å)	Calculated c (Å)	Experimental c (Å)
$GdFe_{12}$	8.423	—	4.801	—
$GdFe_{10}Cr_2$	8.504	8.515	4.77	4.766
$GdFe_{10}V_2$	8.54	8.517	4.796	4.774
$GdFe_{11}Ti$	8.518	8.548	4.81	4.806
$GdFe_{10}Mo_2$	8.66	8.58	4.82	4.805

3.2. The site preference and phase stability

3.2.1. Phase stability for Gd(Fe, T)$_{12}$. From figure 3, it can be seen that an increase in T content causes the crystal cohesive energy of Gd(Fe, T)$_{12}$ to decrease, demonstrating that the addition of these atoms truly stabilizes the structure of GdFe$_{12}$, enabling the Gd(Fe, T)$_{12}$ stable phase to exist. The introduction of Mo and V reduces the GdFe$_{12}$ lattice cohesive energy more significantly than Cr and Ti, indicating that Mo or V will have a higher solubility [4–6]. On the other hand, the calculated results of substitution for Ni, Cu, Co, Sc, Zn, etc increase the system energy. It is therefore inferred that these elements will not stabilize the GdFe$_{12}$ lattice.

3.2.2. Site preference of $T = Cr, Mo, Ti, V$. It can be seen from figure 3 that as the T atom occupies the 8i site, the calculated cohesive energy of GdFe$_{12}$ decreases most significantly; for the 8j site, the energy decreases less, and for the 8f site, the cohesive energies are comparatively high. Thus it is obvious that the T atom will preferentially occupy the 8i site, which is very much consistent with experimental results [4–9]. Some experiments have reported that Ti atoms, in addition to preferentially occupying the 8i site, also attempt to occupy the 8j site. However, the calculated results indicate that the cohesive energy difference between states of Ti occupying the 8i and the 8j sites cannot be ignored. In this calculation, there is no evident trend for the Ti atom to occupy the 8i site and the 8j site simultaneously.

The energy dependence curve as a function of the ternary addition of Mn is convex, in contrast to the concave form seen in other cases. By inference, the structure of GdFe$_{12-x}$Mn$_x$ becomes more and more stable as x increases, so the very stable phase GdMn$_{12}$ would be expected to appear according to this calculation (figure 5). This indicates that the RMn$_{12}$ structure is much more stable than the RFe$_{12}$ structure. This is to some extent consistent with the actual situation [25, 26].

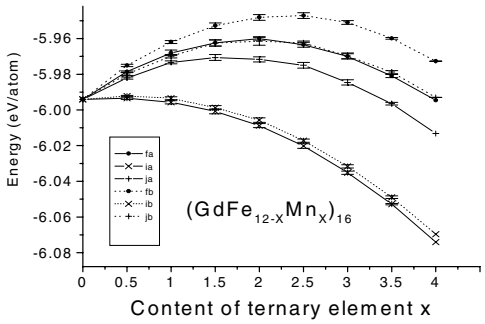

Figure 5. The cohesive energy curve of GdFe$_{12-x}$Mn$_x$.

As regards the site preference and phase stability, a comparison of the calculated results with experiment can be seen in table 3. From table 3, we can see that the evaluated phase stability and site preference are in good agreement with experiment.

4. An intuitive analysis

4.1. Phase stability

'Intuitive' is in some senses the opposite of 'rigorous'; it tells us what kind of visual image we might have, without a complete calculation. Let us first analyse the effect of the ternary element on the structural stability of Gd(Fe, T)$_{12}$. When small ternary additions are involved, the atoms surrounding each ternary atom are mostly Fe atoms. The Gd atom is not nearest

Table 3. The effect of the ternary element on the phase stability and site preference. The notation ⇓ and ⇑ indicates the energy decrease and increase caused by ternary additions.

T	Calculated energy	Phase stability (experimental)	Site preference (calculated)	Site preference (experimental)
Ti	⇓	Yes	8i	8i
V	⇓	Yes	8i	8i
Cr	⇓	Yes	8i	8i
Mo	⇓	Yes	8i	8i
Mn	⇓	Yes	8i	8i
Cu	⇑	No	—	—
Ni	⇑	No	—	—
Zn	⇑	No	—	—
Ag	⇑	No	—	—
Nb	⇓	Yes	8i	8i

neighbour to an atom of its own species, and the occasions on which T atoms are nearest neighbours are truly rare. Therefore, the energy difference between structures before and after substitution is dominated by the difference between $\Phi_{\mathrm{Fe-Fe}}(x)$ and $\Phi_{\mathrm{Fe-T}}(x)$, and the role of $\Phi_{\mathrm{Gd-Gd}}(x)$ and $\Phi_{\mathrm{T-T}}(x)$ can be ignored. The element T can stabilize the R(Fe, T)$_{12}$ structure if $\Phi_{\mathrm{Fe-Fe}}(x) > \Phi_{\mathrm{Fe-T}}(x)$, but cannot play a role in the stability for $\Phi_{\mathrm{Fe-Fe}}(x) < \Phi_{\mathrm{Fe-T}}(x)$. This can explain why elements belonging to the family of V, Ti, Cr, Mn, Nb, Mo, ... stabilize the structure while the elements Ni, Co, Zn, Sc do not.

When large amounts of ternary elements are added, each ternary T atom has a greater chance of being close to rare-earth elements and other T atoms. In this case, the comparisons between $\Phi_{\mathrm{Gd-Fe}}(x)$ and $\Phi_{\mathrm{Gd-T}}(x)$, and between $\Phi_{\mathrm{Fe-Fe}}(x)$ and $\Phi_{\mathrm{T-T}}(x)$, become important. According to our calculation, we find that if $\Phi_{\mathrm{Gd-Fe}}(x) < \Phi_{\mathrm{Gd-T}}(x)$ and $\Phi_{\mathrm{Fe-Fe}}(x) < \Phi_{\mathrm{T-T}}(x)$ over the range 2.4 Å–4.4 Å, both cases will see a decrease in substitution. Therefore, the stability range for the single phase cannot be extended without limit, or the solubility range is the limit. In the case of Mn as the ternary element, we have $\Phi_{\mathrm{Gd-Fe}}(x) > \Phi_{\mathrm{Gd-T}}(x)$, and $\Phi_{\mathrm{Mn-Mn}}(x) < \Phi_{\mathrm{Fe-Fe}}(x)$ over the whole extent of the interatomic distance. This might be why the dependence curve of the total energy of Gd(Fe$_{12-x}$T$_x$) on the content of ternary additions becomes convex and why $GdMn_{12}$ is more stable than $GdFe_{12}$. The above is an intuitive analysis of why some elements can play a role in stabilizing the $GdFe_{12}$ structure, and others cannot. Of course, the real calculation is related to six interatomic potentials $\Phi_{\mathrm{Gd-Gd}}$, $\Phi_{\mathrm{Fe-Fe}}$, $\Phi_{\mathrm{T-T}}$, $\Phi_{\mathrm{Gd-T}}$, $\Phi_{\mathrm{Gd-Fe}}$, and $\Phi_{\mathrm{T-Fe}}$ simultaneously, in a complex relaxation process. It is noted that the important range of interatomic distances for the above discussion is between 2.3 and 4.4 Å (table 4). Also, in this paper, only an energy-minimization process is considered, which is essentially a static method, rather than a molecular dynamics process.

4.2. Site preference

The site preference of a stabilizing atom can be explained simply by carrying out a cluster analysis of the surroundings of the sites 8i, 8j, or 8f in the crystal $GdFe_{12}$ based on a comparison of the interatomic potential curves. As discussed above, all of the interatomic distances are larger than 2.3 Å, and the potential values are most important when the distance is less than 4.4 Å. Therefore, the radius of the cluster is taken as 4.4 Å. It is noted that each $\Phi_{\mathrm{Fe-T}}(x)$ curve (T = Cr, Ti, V, Mo, Ni, Tc, and Zr) intersects the $\Phi_{\mathrm{Fe-Fe}}(x)$ curve at somewhere around 2.7 Å (figure 2). For interatomic distances $x < 2.7$ Å, $\Phi_{\mathrm{Fe-Fe}}(x) < \Phi_{\mathrm{Fe-T}}(x)$, and for this reason the T atom is not substituted for Fe; for $x > 2.7$ Å, $\Phi_{\mathrm{Fe-Fe}}(x) > \Phi_{\mathrm{Fe-Fe}}(x)$, leading to T being preferentially substituted for Fe. On the other hand, each of the curves $\Phi_{\mathrm{Gd-T}}(x)$

intersects $\Phi_{Gd-Fe}(x)$ at approximately 3.4 Å. We are interested in the case of $x < 3.4$ Å, where $\Phi_{Gd-T}(x) > \Phi_{Gd-Fe}(x)$, and it is of no benefit to substitute T for Fe.

On the basis of the potential analysis, the order of preference for substituting T for Fe can be qualitatively estimated by considering the benefit factors as related in table 4, without considering the weight difference.

Table 4. Preference factors for distinct sites for Fe atoms.

Site	No of Fe (<2.7 Å)	No of Fe (2.7–4.4 Å)	No of Gd	Benefit factor
8i	7	24	1	$-7+24-1=16$
8j	10	19	2	$-10+19-2=7$
8f	11	16	2	$-11+16-2=3$

In table 4, the first column represents the number of Fe atoms inside a sphere of radius 2.7 Å, the second column represents the number inside the shell within $r_1 = 2.7$ Å and $r_2 = 4.4$ Å, and the third column corresponds to the centre atom being Gd. We can see that the site preference order for these stabilizing elements in 3d or 4d families is, in most cases, 8i, 8j, 8f. This approximate estimate is in good agreement with experiment. For example, in a Gd(Fe, V)$_{12}$ lattice cell, the distances between Gd atoms and 8i, 8j, and 8f sites are within the range of 2.9–3.3 Å. In this range, the interatomic interaction of Φ_{V-Gd} is much stronger than that of Φ_{Fe-Gd}. Thus V occupying the 8i site is most beneficial in terms of energy minimization, reflected by the site preference substitution behaviour of V. For Gd(Fe, Cr)$_{12}$, the difference in interatomic pair potential between Φ_{Gd-Cr} and Φ_{Fe-Gd} is not significant, so the trend of Cr-site preferential occupation is not evident.

5. Conclusions and discussion

In the present work, the phase stability, site preference, and lattice constants for a series of complex compounds, Gd(Fe, T)$_{12}$, are calculated by using inverted pair potentials based on simple binary systems: Gd–Gd, Fe–Fe, and Gd–T. This implies the applicability of *ab initio* potentials to rare earths. However, it has to be noted that the *ab initio* cohesive energy curve for the 3d elements is somewhat deeper than that obtained from experiment, and should be improved in a future study.

Acknowledgments

We would like to thank Wu Yu, J Zhou, S Q Ho, X L Wang and L Z Cao at Beijing University of Science and Technology for their considerable help with the computation. Many thanks also should go to F M Yang, J L Wang and J K Liang at Institute of Physics in the Chinese Academy of Sciences for interesting discussions and encouragement. This work was supported in part by the National Foundation of Sciences of China, and in part by the National Advanced Materials Committee of China.

References

[1] Yang Y C, Kebe B and James W J 1981 *J. Appl. Phys.* **52** 2077
[2] de Mooij D B and Buschow K H J 1987 *Philips J. Res.* **42** 246
Suski W 1996 The ThMn$_{12}$-type compounds of rare earths and actinides *Handbook on the Physics and Chemistry of Rare Earths* vol 22, ed K A Gschneidner Jr and L Eyring (Amsterdam: Elsevier)
[3] de Boer F R, Huang Ying-kai, de Mooij D B and Buschow K H J 1987 *J. Less-Common Met.* **135** 199

[4] Buschow K H J 1988 *J. Appl. Phys.* **63** 3130
[5] de Mooij D B and Buschow K H J 1988 *J. Less-Common Met.* **136** 207
Buschow K H J 1991 *Rep. Prog. Phys.* **54** 1123
[6] Helmholdt R B, Vleggaar J J M and Buschow K H J 1988 *J. Less-Common Met.* **138** L11
[7] Ohashi K, Tawara Y, Osugi R and Shimao M 1988 *J. Appl. Phys.* **64** 5714
[8] Kim C S, An S Y, Uhm Y R, Lee S W, Kim Y B and Kim C S 1998 *J. Appl. Phys.* **83** 6929
[9] Loong C K, Short S M, Lin J and Ding Y 1998 *J. Appl. Phys.* **83** 6926
[10] Lachevre V, Barbara B, Fruchart D and Pontonnier L 1998 *J. Alloys Compounds* **275–277** 615
[11] Carlsson A E, Gelatt C D and Ehrenreich H 1980 *Phil. Mag.* A **41** 241
[12] Chen N X *et al* 1997 *Phys. Rev.* E **57** R5
[13] Zhang W Q *et al* 1997 *J. Appl. Phys.* **82** 578
[14] Chen N X and Ren G B 1992 *Phys. Rev.* B **45** 8177
[15] Chen N X *et al* 1994 *Phys. Lett.* A **184** 347
[16] Chen N X *et al* 1997 *Phys. Rev.* B **57** 14 203
[17] Ge X J *et al* 1999 *J. Appl. Phys.* **85** 3488
[18] Liu S J, Duan S Q and Ma B K 1998 *Phys. Rev.* B **58** 9705
[19] Williams A R, Kuebler J and Gelatt J R 1979 *Phys. Rev.* B **19** 6094
[20] Moruzzi V L and Sommers C B 1995 *Calculated Electronic Properties of Ordered Alloys* (Singapore: World Scientific)
[21] Monkhorst H J and Pack J D 1976 *Phys. Rev.* B **13** 5188
[22] Anderson D G 1965 *J. Assoc. Comput. Machinery* **12** 547
[23] Rose J M, Smith J R, Guinea F and Ferrante J 1984 *Phys. Rev.* B **29** 2963
[24] Suski W 1996 *Handbook on the Physics and Chemistry of Rare Earths* vol 22, ed K A Gschneidner Jr *et al* (New York: Elsevier) ch 149
[25] Balammaane H, Halicioglu T and Tiller W A 1992 *Phys. Rev.* B **46** 2250
[26] Burzo E and Vadeanu S T 1979 *J. Less-Common Met.* **66** 111